



HYDROTHERMALLY GROWN ZnO/rGO AND ZnO/PANI NANOHYBRIDS: COMPARATIVE STUDY ON THEIR ELECTRICAL CONDUCTANCE

Nisha T. Padmanabhan¹, Rose Santhosh², Annett Antony², Ushamani Mythili*²

¹Inter University Centre for Nanomaterials and Devices (IUCND), Cochin University of Science and Technology, Kerala, India

²Department of Chemistry and Centre for Research, St. Teresa's College (Autonomous), Ernakulam, Kerala, India

*Corresponding author: ushanim@teresas.ac.in

Received: 12-09-2022; Accepted: 06-11-2022; Published: 30-11-2022

© Creative Commons Attribution-NonCommercial-NoDerivatives 4.0 International License <https://doi.org/10.55218/JASR.2022131002>

ABSTRACT

The unique properties of Zinc Oxide, Graphene and their nanocomposite have enabled them to fabricate many optoelectronic devices which offer advantages like light weight, good stability and optical transparency. Conducting polymer/graphene hybrids are also a major class of composite materials for the fabrication of donor/acceptor based electronic devices. In this paper we report the synthesis, characterization and conductivity measurements in ZnO/rGO and ZnO/PANI binary nanohybrids. ZnO nanotops are synthesized by low temperature hydrothermal method, graphene oxide (GO) by modified Hummer's Method, reduced graphene oxide (rGO) by hydrothermal *in situ* reduction technique and PANI from aniline by chemical polyoxidation reaction. ZnO/rGO nanohybrid is prepared by hydrothermal treatment of ZnO and GO, whereas ZnO/PANI by *in-situ* oxidative polymerization of aniline in presence of ZnO. All the materials were characterized using SEM, TEM, XRD, UV-Vis, IR&TGA. The as-synthesized samples were dispersed in IPA, coated on quartz glass using spin-coating technique, and dark conductivity measurements were done.

Keywords: Polyaniline, Graphene, Nano hybrids, Zinc Oxide, Graphene oxide, Hydrothermal method.

1. INTRODUCTION

ZnO is a wide direct bandgap semiconductor with large exciton binding energy at room temperature. The absorption of ZnO can be tuned within the visible spectral region by controlling the intrinsic defect levels and the intrinsic defect levels can create localized states within the band gap, which influences the optical absorption and the carrier dynamics [1-3]. The modification of ZnO with graphene is a novel and green approach to control the morphology, surface defect states and photoresponse of ZnO nanocrystals. Moreover, graphene-semiconductor hybrid materials have been identified as good candidates for photonic and optoelectronic applications like solar cells, photo-detectors, optical limiters and ultra-fast lasers [4]. This is due to the excellent electronic properties of graphene and its prominent capability to store and shuttle photogenerated electrons from the bandgap excitation of semiconductors upon light irradiation.

ZnO-graphene hybrids can be prepared by either an *ex situ* or *in situ* method. In the first approach, ZnO with desired shape and size are synthesized in advance. It can

bind to the surface of graphene by non-covalent interaction and this *ex situ* approach can be carried out by epitaxial growth, chemical deposition or self-assembly. The *in-situ* growth method is widely used for the synthesis of ZnO-graphene hybrids, graphene oxide (GO) is used as the precursor for graphene [5]. During the nucleation of ZnO, simultaneous reduction of GO occurs. By the fabrication of ZnO-graphene hybrid systems, we can control the morphology, surface defect states and the photoresponse of ZnO nanocrystals.

Among various conducting polymers, polyaniline is the most attractive conductive polymer because of the presence of the reactive -NH- groups in polymer chain and used in broad applications such as batteries, sensors and electronic devices, super capacitors and corrosion protection in organic coatings and due to its physical and chemical properties, good electrical conductivity (p-type), high environmental stability, low cost and light weight, flexibility, facile fabrication and possibility of both chemical and electrochemical synthesis. Electrical conductivity of polyaniline is very important parameter and it could be modified by the addition of inorganic

fillers. PANI-ZnO nanocomposites exhibit many new properties such as electrical, optical, catalytic and mechanical properties that the single material does not have [6-8]. In this paper we report the synthesis, characterization and conductivity measurements in ZnO/rGO and ZnO/PANI binary nanohybrids.

2. MATERIAL AND METHODS

2.1. Chemicals

Zinc acetate dihydrate ($\text{Zn}(\text{Ac})_2 \cdot 2\text{H}_2\text{O}$), polyethylene glycol (PEG, mol. wt. 3,500 - 5,500) sodium hydroxide (NaOH), 98% sulfuric acid (H_2SO_4), 65% nitric acid (HNO_3) were purchased from Merck India. Aniline, 30% hydrogen peroxide (H_2O_2), toluene sulphonic acid (TSA), ammonium peroxydisulphate (APS), Dimethyl sulphoxide (DMSO) was received from Spectrochem, India. Graphite powder (particle size $< 20\mu\text{m}$) was obtained from Sigma Aldrich. Potassium permanganate (KMnO_4) was obtained from Universal Laboratories, India. All the chemicals were used as received without further purification.

2.2. Synthesis

Wurtzite ZnO nanotops is prepared by a low temperature hydrothermal method [9] by first stirring 0.216g Zinc acetate dehydrate with 100ml 0.05% PEG solution. After 24 h, NaOH solution was added dropwise till pH of the solution reached 11. It was then transferred to a 100 ml Teflon-lined stainless steel Autoclave and kept in an oven at 100°C for 7 h. The white precipitate obtained was filtered, washed and dried at 100°C under vacuum. GO was prepared by modified Hummers method [10-12] from Graphite powder on treating with conc. H_2SO_4 , KMnO_4 and finally with 30% H_2O_2 and water. The dispersion was washed several times with deionised water, centrifuged and dried under vacuum at 60°C .

ZnO/rGO nanohybrid was prepared hydrothermally by first dispersing ZnO and GO (in proportion 0.05:0.05) in DMSO, then transferring the dispersed solution to a 50ml Autoclave and treating at 100°C for 7 h, and ZnO/PANI nanohybrid (in proportion 0.05:0.2) was prepared by the *in situ* polymerization of aniline in the presence of ZnO through chemical polyoxidation reaction. Aniline and APS were added after the complete dispersion of ZnO in 40ml (1M) TSA solution, and stirred for 9 h. The precipitate was filtered, washed and dried in vacuum at 60°C .

2.3. Fabrication

Thin layers of the as-prepared samples were fabricated on clean FTO glass slides. 0.5 mg/ml of ZnO, ZnO/rGO or ZnO/PANI was dispersed in IPA by ultrasonication. This uniform dispersion was spin coated on FTO by a two-step process at 500 rpm for 120 s and 3000 rpm for 30 s and the coated films were dried at room temperature. For the dark conductivity measurement, all the films were coated nine times continuously.

2.4. Characterization

Crystallographic shape, structure and size of the prepared samples were investigated by X-ray diffraction (XRD, PANalytical X'Pert Pro) and transmission electron microscope (TEM, JEOL JEM-2100) images. Electrical property was studied using confocal micro Raman Spectrometer (Horiba JobinYvon Lab RAM HR), structural features of the samples using Fourier transform infrared spectroscopy (FTIR) (JASCO FT/IR-4100), optical properties using UV-visible absorption (Thermo Scientific Evolution 201), and thermal decomposition patterns using thermo gravimetric analysis (TGA, TA Instruments Q50). Dark conductivity measurement was done using Nano voltmeter.

3. RESULTS AND DISCUSSION

The morphology of the synthesized ZnO nanoparticles had a cone-shaped structure as it is evident from the TEM image (Fig. 1a). The XRD diffractogram of the so prepared ZnO nanotops (Fig. 1b) shows all the diffraction peaks corresponding to the planes of hexagonal wurtzite structure (JCPDS file no. 36-1451). The average crystallite size of ZnO is calculated using Scherrer equation and is found to be 24nm. UV-Vis spectra of ZnO (Fig. 1c) shows a sharp absorption peak at 361 nm showing a blue shift relative to the bulk exciton absorption (380 nm) as a result of the quantum size effect; and a band gap of 3.2 eV in the tauc plot (inset of Fig. 1c).

The XRD diffractograms of the prepared samples (Fig. 2) show that there is a characteristic peak of (001) plane in GO at $2\theta=10.54^\circ$ is shifted to 25.2° in ZnO-rGO which attributes to the complete reduction of GO to rGO. ZnO-PANI is more of an amorphous nature than ZnO-rGO, and the peak at $2\theta=21.6^\circ$ is the characteristic peak of (020) plane in PANI.

The morphology and crystal structures of the prepared samples are studied by HR-SEM and TEM images. The SEM micrograph of PANI shows rod-like structure (Fig.

3a). PANI is having the same morphology in the hybrid ZnO-PANI as shown by the TEM image (Fig. 3b) with the dark patches corresponding to ZnO nanoparticles. Whereas the TEM micrograph of ZnO-rGO (Fig. 3c) has

ZnO nanoparticles embedded within the transparent sheets of graphene. Both binary hybrids have an even distribution of ZnO with graphene or PANI.

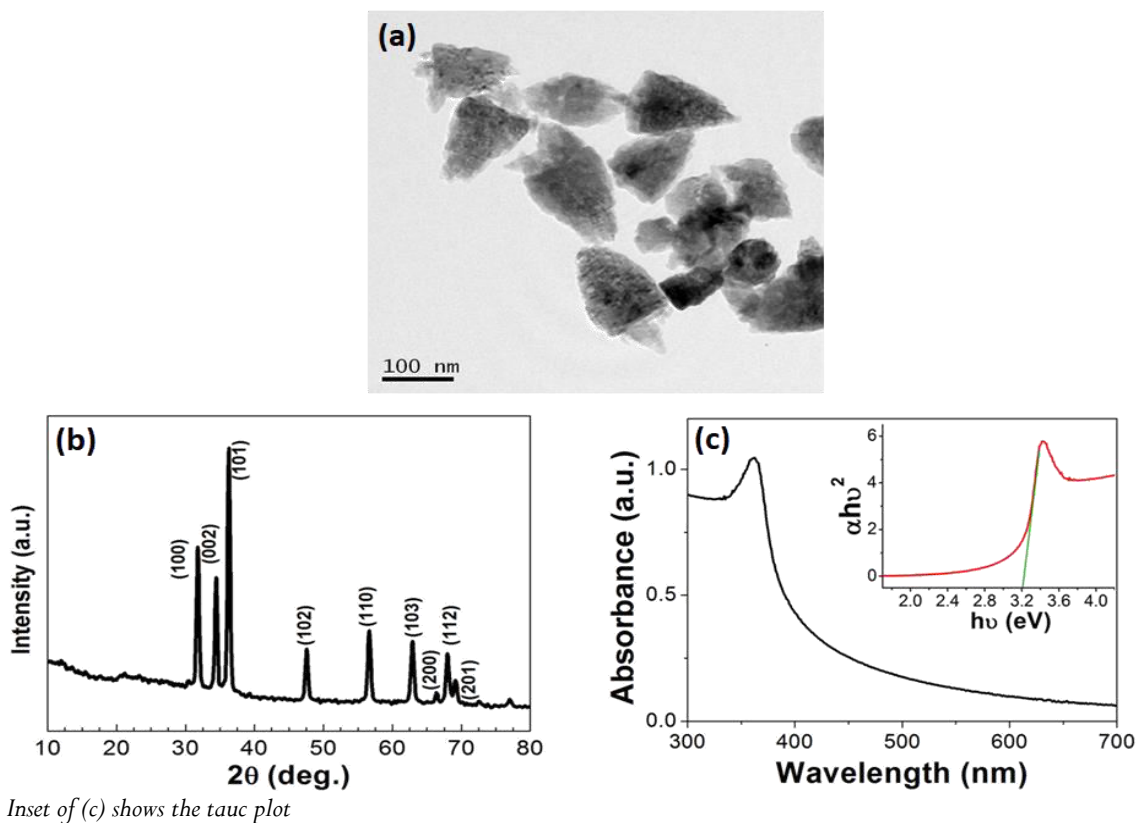


Fig. 1: (a) TEM, (b) XRD Spectra, and (c) UV-Vis Spectra of as-synthesized ZnO nanoparticles

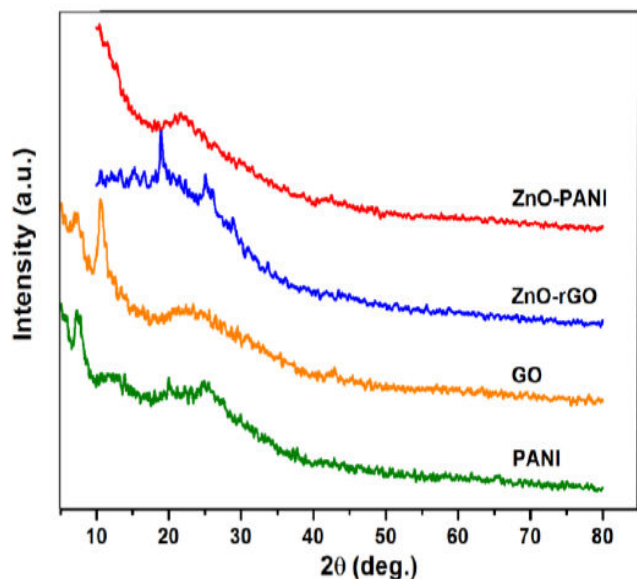


Fig. 2: XRD diffractograms of prepared PANI, GO, ZnO-rGO and ZnO-PANI

Fig. 4a shows all characteristic IR vibrations of PANI at 1630, 1484, 1305, 1140 and 571 cm^{-1} corresponding to C=C stretching of quinonoid rings, C=C stretching of benzenoid rings, C-N stretching, aromatic C-H in-plane bending, and C-H out-of-plane vibrations, respectively. ZnO-PANI (Fig. 4b) shows the characteristic peaks of polyaniline, but are shifted to lower wave number side. The peaks corresponding to GO are significantly reduced in the hybrid ZnO-rGO indicating the removal of functional groups during the hybrid formation.

The decomposition patterns of the samples are studied using thermo gravimetric analysis. As shown in Fig. 5, ZnO-PANI has greater thermal stability giving a residue of ~62%, than ZnO-rGO. The major weight loss of all samples is between 180 to 300°C which shows that the samples have maximum efficiency below this temperature range.

The DC conductivity in the dark is measured for the as-prepared ZnO, ZnO-PANI and ZnO-rGO. Table 1

shows the obtained data. Both ZnO-rGO and ZnO-PANI binary hybrids has increased conductivity than compared to ZnO. This is due to the hybridization of ZnO with that of either PANI or Graphene. Whereas

the better response of ZNO-rGO ($0.519 \mu\text{A}$) than ZnO-PANI ($0.425 \mu\text{A}$) is due to the characteristic property of Graphene.

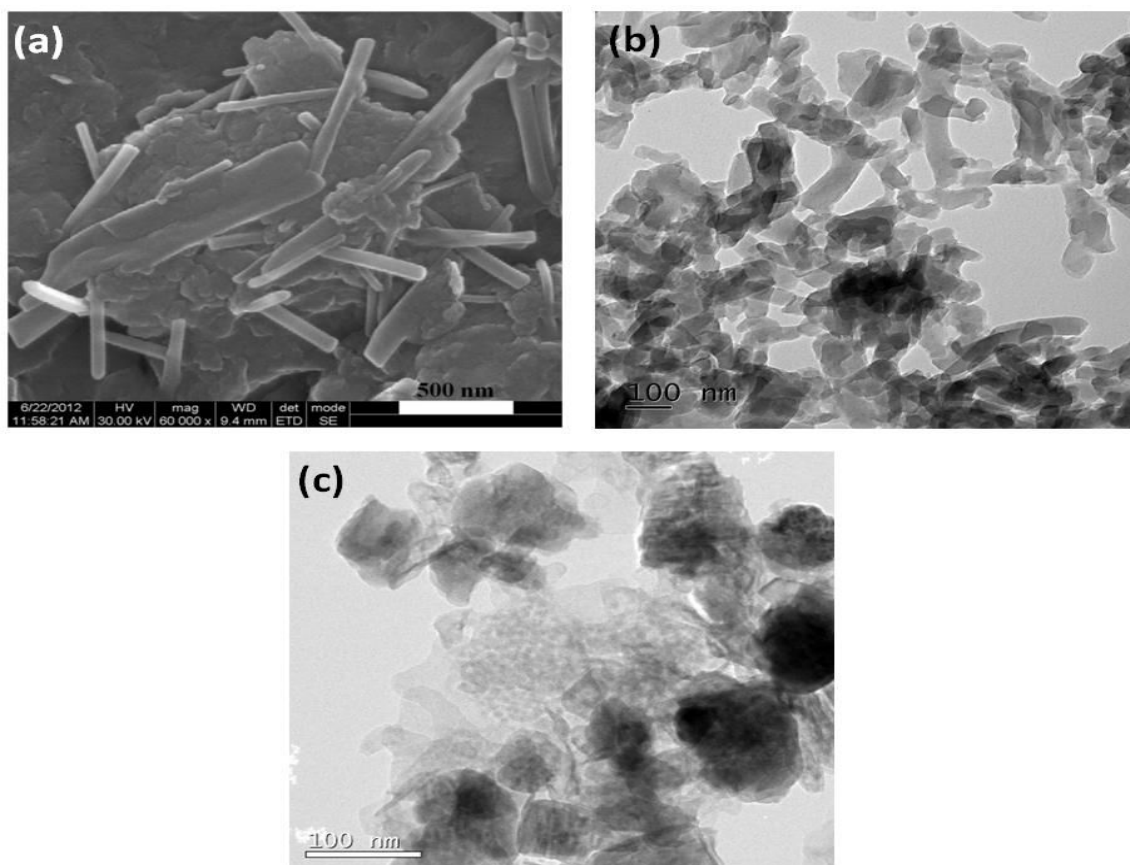


Fig. 3: SEM micrograph of (a) PANI, (b) TEM micrographs of ZnO-PANI and (c) ZnO-rGO

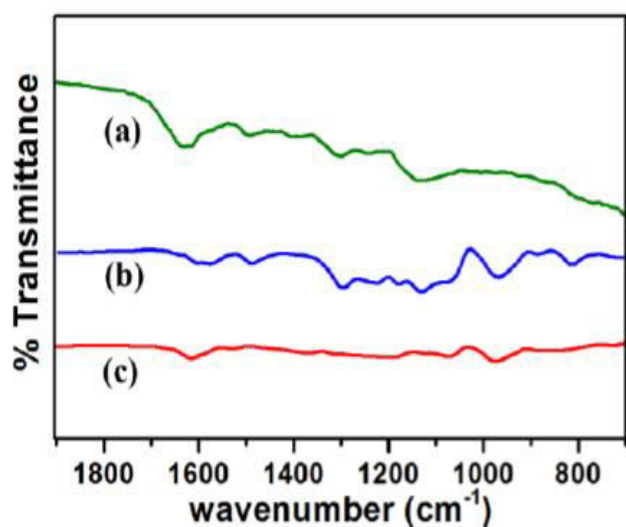


Fig. 4: FTIR spectra of PANI (a), ZnO-PANI (b), ZnO-rGO (c)

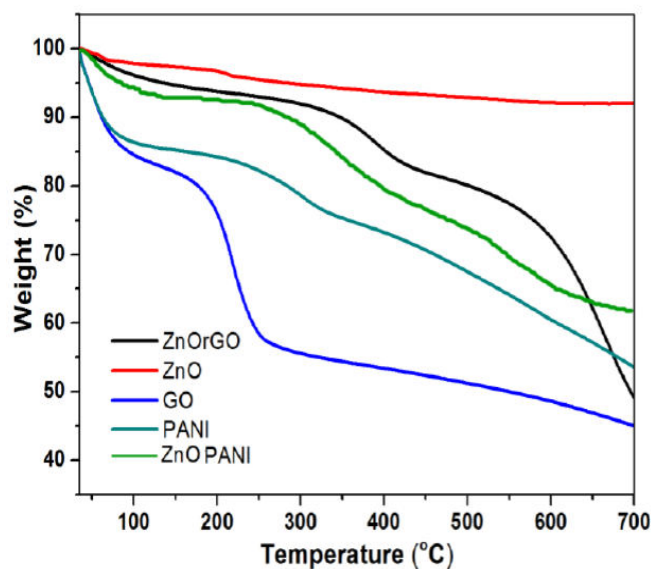


Fig. 5: Thermographs of as-prepared samples

Table 1: Conductivity in dark for the samples

Samples	Conductivity (μA)
ZnO	0.378
ZnO-PANI	0.425
ZnO-rGO	0.519

4. CONCLUSION

In summary, ZnO nanotops, GO, PANI were synthesized by suitable facile methods. ZnO-rGO synthesized by hydrothermal method, where GO is *in-situ* reduced and ZnO-PANI by chemical polyoxidation method in which aniline is *in-situ* polymerized. These synthesized samples were characterized by XRD, SEM, TEM, IR, UV and TGA analysis. Conductivity in the dark is measured for ZnO, ZnO-rGO and ZnO-PANI by coating them on a glass substrate. A better response of conductivity is found for ZnO-rGO than for ZnO-PANI and ZnO.

Conflict of interest

None declared

5. REFERENCES

- van Dijken, EA. Meulenkaamp, D. Vanmaekelbergh, A. Meijerink. *J. Phys. Chem. B*, 2000; **104(8)**:1715-1723.
- Aswathi KS, Alejandro GG, Lorenzo DM, Nicolas T, Javier HF, Daniele C, et.al. *Nanoscale Adv*, 2021; **3**:214–222.
- Zhang Ke-Xin, Yao Cheng-Bao, Wen Xing, Li Qiang-Hua, Sun Wen-Jun. *RSC Adv*, 2018; **8**:26133–26143.
- Bonaccorso F, Sun Z, Hasan T, Ferrari AC. *Nature Photonics*, 2010; **4**:611–622.
- Kavitha MK, John H, Gopinath P, Philip R. *J. Mater. Chem*, 2013; **1**:3669-3676.
- Mostafaei A, Zolriasatein A. *Progress in Natural Science: Materials International*, 2012; **22(4)**:273–280.
- Baig MF, Safiullah M, Husain J, Raghu N. *Int. Journal of Engineering Research and Application*, 2016; **6(9)**:07-11.
- Dhole SG, Dake SA, Prajapati TA, Helambe SN. *Science Direct Procedia Manufacturing*, 2018; **20**:127-134.
- Mohan S, Vellakkat M, Aravind A, U Reka. *Nano Express*, 2020; **1(3)**:1-14.
- Kavitha MK, Pillai SC, Gopinath P, John H. *J. Environ. Eng*, 2015; **3**:1194-1199.
- Zaaba NI, Foo KL, Hashim U, Tan SJ, Liu Wei-Wen, Voon CH. *Science direct Procedia Engineering*, 2017; **184**:469–477.
- Lucas GPT, Ludmila da Silva C, Barbara de Salles Macena da Cruz, Fernanda FG, Matheus PR, Renata AS et al. *Journal of Material Research and Technology*, 2022; **18**: 4871-4893.